Original Research Paper

BioPerine Encapsulated Nanoformulation for Overcoming Drug-Resistant Breast Cancers

Sindhu C Pillai[a], Ankita Borah[a], Amandeep Jindal[b], Eden Mariam Jacob[a], Yohei Yamamoto[b], D. Sakthi Kumar[a],*

[a] *Bio-Nano Electronics Research Centre, Graduate School of Interdisciplinary New Science, Toyo University, Saitama 350-8585, Japan*
[b] *Department of Materials Science, Faculty of Pure and Applied Sciences, University of Tsukuba, Tsukuba, Ibaraki 305-8573, Japan*

ARTICLE INFO

ABSTRACT

The evolving dynamics of drug resistance due to tumor heterogeneity often creates impediments to traditional therapies making it a challenging issue for cancer cure. Breast cancer often faces challenges of current therapeutic interventions owing to its multiple complexities and high drug resistivity, for example against drugs like trastuzumab and tamoxifen. Drug resistance in the majority of breast cancer is often aided by the overtly expressed P-glycoprotein (P-gp) that guides in the rapid drug efflux of chemotherapy drugs. Despite continuous endeavors and ground-breaking achievements in the pursuit of finding better cancer therapeutic avenues, drug resistance is still a menace to hold back. Among newer therapeutic approaches, the application of phytonutrients such as alkaloids to suppress P-gp activity in drug-resistant cancers has found an exciting niche in the arena of alternative cancer therapies. In this work, we would like to present a black pepper alkaloid derivative known as BioPerine-loaded chitosan (CS)-polyethylene glycol (PEG) coated polylactic acid (PLA) hybrid polymeric nanoparticle to improve the bioavailability of BioPerine and its therapeutic efficacy in suppressing P-gp expression in MDA-MB 453 breast cancer cell line. Our findings revealed that the CS-PEG-BioPerine-PLA nanoparticles demonstrated a smooth spherical morphology with an average size of 316 nm, with improved aqueous solubility, and provided sustained BioPerine release. The nanoparticles also enhanced *in vitro* cytotoxicity and downregulation of P-gp expression in MDA-MB 453 cells compared to the commercial inhibitor verapamil hydrochloride, thus promising a piece of exciting evidence for the development of BioPerine based nano-drug delivery system in combination with traditional therapies as a crucial approach to tackling multi-drug resistance in cancers.

* Corresponding author. Bio-Nano Electronics Research Centre, Graduate School of Interdisciplinary New Science, Toyo University, 2100 Kujirai, Kawagoe, Saitama, 350-8585, Japan. Tel.: +81 492 39-1636/1375.
E-mail address: sakthi@toyo.jp (D.S. Kumar).

1. Introduction

Recurring clinical issues associated with breast cancer treatment is the development of drug resistance. Reports of women detected with early-stage breast cancer might have recurrent disease prognosis and therapeutic resistance that can be either *de novo* or acquired [1,2]. Breast cancer is described to be a heterogeneous disease where the tumor profile is clinically divided into three basic subtypes based on the expression of (i) estrogen receptor and progesterone (ER/PR), (ii) human epidermal growth factor receptor 2 (HER-2), and (iii) triple-negative breast cancer which expresses none of these hormone receptors. Each breast cancer subtype command different treatment regimen often used in combination with traditional chemotherapies [3]. The molecular mechanisms associated with drug resistance in these three subtypes comply to be complex, different and not mutually exclusive. With respect to hormone receptor-positive breast cancer, its accounted to be the cause of 70% of all breast cancer cases reportedly having high expression of estrogen receptor [4]. Endocrine therapy is the go-to front-line therapy for this subtype breast cancer and can develop resistance towards it in patients with metastatic ER-positive cancers [2,4]. Similar tendencies of displaying resistance towards endocrine therapy have been established for HER-2 positive cancers leading to poorer clinical outcomes [5]. HER-2 positive breast cancer patients in the long run often develop *de novo* resistance to the targeted therapy of trastuzumab [6]. The last subtype in this category which is triple-negative breast cancer, reports nil expression of all the three hormone receptors and limited to therapeutic modalities. The available options against this subtype are the use of taxanes and anthracyclines along with surgical approaches [7]. Triple-negative breast cancer cases develop resistance to taxanes and anthracyclines due to rapid drug efflux leading to decreased intracellular drug concentration. The rapid drug efflux is mediated by ATP-binding cassette (ABC) family of drug transporters that utilize ATP hydrolysis to translocate substrates and their increased expression concurs with dissatisfactory clinical outcomes irrespective of any subtype [8]. P-glycoprotein (P-gp) is one of the widely-studied ABC transporters encoded by (ABCB1) multi-drug resistance 1 (MDR1) gene that efflux taxanes and anthracyclines culminating in resistance [9].

In this paper, we focus on the development of a therapeutic strategy directed towards the downregulation of P-gp in drug-resistant breast cancers to reduce the drug efflux from the breast cancer cells. Several clinical trials of P-gp inhibitors have met with limited success [10] contributed mainly due to drug interactions, toxicities and insufficient clinical design [11]. A recent study made by the efforts of Nanayakkara AK et al. identified three targeted P-gp inhibitors through computational high throughput drug docking studies and elucidated increased efficacy in inhibiting P-gp and improved accumulation of chemotherapeutics inside two and three-dimensional cell cultures resistant ovarian and prostate cancer cell lines [12]. In the lines of developing innovative targeted therapies against P-gp nutraceutical/dietary compounds have proven to be safer alternatives in reversing multidrug resistance in cancer. Among the plethora of natural dietary compounds available for P-gp inhibition, [13] piperine, a major plant alkaloid present in black pepper and long pepper accounted enhanced inhibitory P-gp efflux activity in a number of drug-resistant cancer cell lines [14,15]. From inhibiting drug transporters such as P-gp, eliciting anti-inflammatory, anti-arthritic, anti-tumor to being used as a bio enhancer with various natural compounds [16,17] and therapeutically diverse compounds the effects of piperine is wide and well-established. Several independent researchers have divulged into the improved chemo sensitizing effect of conventional chemotherapeutics after piperine administration [18]. However, clinical translation of piperine has been hindered due to its hydrophobicity that requires continuous administration to maintain the therapeutic concentration. The administration of piperine via drug delivery systems aided by nanoparticles (NPs) could contribute a better retention of the compound intracellularly and perform its inhibitory functions. Piperine co-delivered with other dietary compounds such as curcumin in the chitosan-zein NPs have been studied in the *in vitro* efficacy of neuroblastoma cells [19]. Another study demonstrated co-delivery of rapamycin and piperine inside PLGA NPs and reported its therapeutic efficacy in breast cancer cells [20].

The current study aims to develop a polylactic acid (PLA) based NP drug delivery system encapsulating BioPerine an alkaloid compound sourced out of piperine and the NP further coated with chitosan and polyethylene glycol (PEG) as an additional surface modification to downregulate P-gp activity in a triple-negative drug-resistant breast cancer cell line MDA-MB 453. The development of nano-drug delivery carriers for piperine delivery improved its stability and bioavailability. The choice of nanocarrier for piperine delivery ranged from protein, polymers (PLA and PEG), polysaccharides (chitosan), and other natural biomacromolecules which offers excellent biocompatibility, biodegradability and non-toxic properties [21,22]. One of the widely used FDA-approved polymers manufactured under current good manufacturing practice (cGMP) regulation for biomedical applications is PLA [23,24]. We chose PLA as a nanocarrier for BioPerine delivery against drug-resistant breast cancer due to its above-mentioned properties with adjustable physical and mechanical characteristics as reported previously in extensive studies citing its advantages as a drug delivery carrier. PLA NPs offer flexibility in its size, shape, highly reproducible with minimum expenditure [25]. PLA NPs can encapsulate active pharmaceutical ingredient (API) like BioPerine successfully into its polymeric matrix and achieve prolonged therapeutic drug release profile [26]. PLA once reaches inside the body, it breakdowns into monomeric units of lactic acid via carbohydrate metabolism. These NPs could be easily prepared by the common techniques of solvent evaporation, solvent displacement, salting out and solvent diffusion [27]. PLA NPs also offers excellent surface modifications such as surface coating with other hydrophilic biomaterials like chitosan and PEG. Chitosan is a cationic polymer having bio adhesive, biocompatible, biodegradable and low toxicity properties often used to coat NPs for curbing the

phagocytic effects of the reticuloendothelial system (RES) while enhancing the penetration of large molecules across mucosal surfaces [28,29]. The additional PEG coating improves the biocompatibility of chitosan and minimizes the plasma proteins adsorption on the BioPerine-PLA NPs. PEG coating on NPs substantially improves in the evasion of NPs by RES by shielding them and forming a hydrated outer shell [30]. The use of chitosan and PEG simultaneously to coat PLGA NPs with various concentrations of chitosan and PEG have been discussed in detail by Parveen S et al [31]. This surface modification by chitosan and PEG is used to achieve longevity and better circulation of the therapeutic chitosan-PEG-BioPerine-PLA nanoparticles (CS-PEG-Bio-PLA NPs) to carry out its intended function in the triple-negative breast cancer cells. We also sought to find out the comparative therapeutic efficacy of CS-PEG-Bio-PLA NPs against the commercial P-gp inhibitor verapamil hydrochloride (Ver). Ver is a first-generation P-gp inhibitor may act well in a wide range of cancers such as non-small cell lung cancer, colon cancer and neuroblastoma [32,33] combined with other chemotherapy drugs however possess some unwanted side effects such as exposed to higher risks of ductal and lobular cancer with additional blockade of other calcium channels. Henceforth safer alternatives such as CS-PEG-Bio-PLA NPs could warrant better treatment strategies for P-gp inhibition.

2. Materials and methods

2.1. Materials

Acid terminated polylactic acid (PLA, MW 10,000–18,000), chitosan (MW 50 000–190 000 Da, 75%–85% degree of acetylation), polyethylene glycol (PEG) (MW 8500-11,500) and polyvinyl alcohol (PVA) were purchased from Sigma Aldrich (St. Louis, USA). Chloroform and dimethyl sulfoxide (DMSO) was purchased from Kanto Chemicals (Japan). Drugs including Bioperine was a kind gift from Sami Sabinsa Group, Sami Labs (Tokyo, Japan), verapamil hydrochloride (Ver) and doxorubicin hydrochloride (Dox) was purchased from TCI (Japan) and Cayman Chemicals (USA), respectively. Cell culture reagents including Leibovitz's L15 medium, Trypsin-EDTA (0.25%), penicillin (5000 U/ml)/streptomycin (5000 µg/ml), and phosphate buffer saline (PBS, pH 7.4) were procured from Gibco (Life Technologies). Cellular assay kit Presto Blue was procured from Invitrogen (USA). Phalloidin-iFluor 647 reagent, DCFDA/H2DCFDA cellular ROS assay kit, P-gp primary antibody and goat anti-rabbit Alexa-Fluor 594 secondary antibody was procured from Abcam.

2.2. Cell culture maintenance

MDA-MB 453 a triple-negative multi-drug resistant breast cancer cell line was purchased from American Type Culture Collection (USA). The cell line was cultured and maintained in L15 medium supplemented 10% FBS and 1% penicillin/streptomycin in 37 °C incubator till confluent. Media is changed accordingly every 2-3 d.

2.3. Preparation of Chitosan-PEG coated PLA NPs encapsulating BioPerine

The fabrication of chitosan-PEG coated PLA NPs encapsulating BioPerine (CS-PEG-Bio-PLA NPs) was adopted from Parveen S et al. with slight modifications [31]. Briefly, 20 mg of PLA and 2 mg of BioPerine were mixed with 3 ml of chloroform and kept on magnetic stirring to form primary emulsion. In another beaker 2% (w/v) PVA aqueous solution, 0.2% (w/v) chitosan in 1% glacial acetic acid solution (filtered) and 20% (w/v) PEG aqueous solution was added and stirred for a while. The PLA-BioPerine organic mixture was then added dropwise to the PVA-chitosan-PEG aqueous mixture while on rapid stirring. This emulsion was then sonicated for 3 min using a probe sonicator to create a fine milky-white emulsion and left for overnight evaporation of chloroform. Following day, the NPs were collected upon centrifugation (58 × 100 G, 30 min). CS-PEG-Bio-PLA NPs were washed 3–4 times with Milli Q water, freeze-dried, and the lyophilized NPs were stored at -20 °C till further use. Coumarin-6-loaded fluorescent NPs were also prepared similarly for their later use in studying the intracellular uptake in cancer cells.

2.4. Encapsulation efficiency

The encapsulation of BioPerine inside the PLA NPs was measured by an indirect method as described by Amini Y et al. [34]. The supernatant was collected during the synthesis of CS-PEG-Bio-PLA NPs at each washing step which was then used to analyze the BioPerine absorbance λ_{max} at 342 nm by UV-Vis spectroscopy. The obtained absorbance value was then used to quantitate the amount of free BioPerine present in the supernatant using the BioPerine calibration curve equation. The encapsulation efficiency was calculated using the following formula (Eq. 1):

$$Encapsulation\ Effciency\%$$
$$= \frac{Mass\ of\ initial\ BioPerine\ taken\ for\ NP\ Synthesis - Mass\ of\ free\ BioPerine\ in\ the\ supernatant}{Mass\ of\ initial\ BioPerine\ taken\ for\ NP\ Synthesis}$$
$$\times\ 100 \tag{1}$$

2.5. Surface morphology and size distribution analysis

The shape and surface morphology of CS-PEG-Bio-PLA NPs was analyzed using scanning electron and transmission microscopy. For SEM analysis, CS-PEG-Bio-PLA NPs were dispersed in Milli Q water and 10 µl of the water dispersed NPs was drop cast on a clean Silicon (Si) wafer and left for vacuum drying. The dried sample is sputter-coated with platinum (Pt) for 40 sec observation. Before TEM analysis, the water dispersed NPs were dropped onto a previously hydrophilized TEM grid and left for vacuum drying. TEM observation was conducted on a Hitachi high-technology model H7650 operating at an accelerating voltage of 80 kV. Dynamic light scattering (DLS) and zeta potential measurements were carried out using a disposable sizing cuvette and dip cell in Malvern Nano ZS zeta sizer.

2.6.   Surface chemistry analysis

The surface chemistry of PLA NPs and CS-PEG-Bio-PLA NPs was analyzed by XPS (JEOL JPS 9010TR Nano Science) using Al kα monochromatic transmission mode at a base pressure of 10^{-9} Torr. Chitosan, BioPerine and PEG samples were also used to check the chemical composition and compare it with CS-PEG-Bio-PLA NPs spectra. The binding energy of the wide scan spectra for all the samples recorded from 0 to 1000 eV.

2.7.   Chemical interaction by fourier transform infrared (FTIR) spectroscopy

The chemical interaction and chemical bonding patterns of the components present in CS-PEG-Bio-PLA NPs were investigated by FTIR spectrometer (Nicolet iS50FT-IR, JASCO FT/IR-4200) and the spectra were recorded in the resolution of 4 cm^{-1} ranging from 4000 to 400 cm^{-1}. PLA NPs, chitosan, BioPerine, and PEG samples were also analyzed for comparison with CS-PEG-Bio-PLA NPs.

2.8.   Nature of drug in NPs by X-ray diffraction study

The patterns of pure BioPerine, PEG, chitosan, PLA NPs, and CS-PEG-Bio-PLA NPs were obtained using the X-ray diffractometer (Rigaku, Miniflex 600) with a Cu (kα) radiation source at 40 kV and 15mA. The scan angle was changed between 5° and 50° with a scan size of 2 theta.

2.9.   In vitro drug release studies

Briefly, 2 mg CS-PEG-Bio-PLA NPs were dissolved in 10 ml PBS buffer (pH 7.4 and 6.5) supplemented with 50% FBS and divided into 10 Eppendorf tubes each maintaining a concentration of 200 μg/ml. The addition of FBS in the PBS buffer mimics the serum physiological conditions. The tubes were kept inside a shaking incubator at 37 °C for 4 d. At pre-determined time intervals, the tubes were taken out one by one, centrifuged at 130×100 G for 30 min. The supernatant was then subjected to measuring the absorbance of released BioPerine by UV-Vis spectroscopy. The amount of released BioPerine is quantified using the calibration curve equation for BioPerine. The release percentage of BioPerine was calculated using Eq. 2.

$$BioPerine\ Release\% = \frac{Released\ BioPerine\ from\ NPs}{Total\ Bioperine\ encapsulated\ inside\ NPs} \times 100 \quad (2)$$

2.10.   Intracellular uptake of fluorescent CS-PEG-Coumarin 6-PLA NPs

The internalization of NPs inside the cells and tissues could be traced using fluorescent NPs. We performed the cellular uptake of coumarin-6 loaded PLA-chitosan-PEG NPs in MDA-MB 453 breast cancer cells by confocal laser scanning microscope (CLSM) (Nikon A1 Plus). The MDA-MB 453 cells were sub-cultured and seeded onto confocal dishes at a concentration of 5000 cells. The cells upon reaching confluency were incubated with the coumarin-6 loaded PLA-chitosan-PEG NPs for 4 h and 12 h. Upon completion of the incubation period, the NPs were removed, cells were washed thrice with PBS (pH 7.4). Cells were then fixed with 4% formaldehyde for 10-20 min, followed by washing with PBS. 0.1% Triton X-100 was then added to the fixed cells for cell membrane permeabilization. The cells were stained with phalloidin-iFluor 647 reagent for 1 h to co-localize the actin filaments. NucBlue Live Ready probes were used to stain the nucleus. Coumarin-6 fluoresces under the FITC laser channel (Ex/Em = 488 nm/ 525 nm) while phalloidin-iFluor 647 reagent at (Ex/Em = 650 nm/665 nm).

2.11.   PrestoBlue cell viability assay

The cytotoxicity analysis of the BioPerine-loaded PLA-chitosan PEG NPs towards the MDA-MB 453 cells was performed using Presto Blue resazurin based reagent. We carried out a dose and time-dependent comparative analysis of CS-PEG-Bio-PLA NPs with the commercially available P-gp inhibitor Ver. We also sought to evaluate the desensitization effects of CS-PEG-Bio-PLA NPs and Ver on the P-gp activity of MDA-MB 453 cells followed by treating the cells with a conventional chemotherapeutic drug Dox We speculate an enhanced therapeutic efficacy on the MDA-MB 453 cells with this combination regimen.

The cells were seeded in a 96-well plate at 5000 cells/well and grown till confluent. We chose to use the reported IC_{50} concentration of Ver (29 μM) and Dox (25 μg/ml) on the MDA-MB 453 cells [35]. As for CS-PEG-Bio-PLA NPs we chose six different concentrations (25, 50, 100, 200, 500 and 1000 μg/ml) to evaluate its inhibitory capacity on the P-gp. For combination regimen, cells were pre-treated with Ver (29 μM) and CS-PEG-Bio-PLA NPs (500 and 1000 μg/ml) for 24 h to downregulate the P-gp activity. In the next day, the drug and NPs were removed and the cells were administered with Dox(25 μg/ml) for 24-48 h. After each incubation period, the NPs and drugs were aspirated, fresh medium and 10% of Presto Blue reagent were added to the cells. The fluorescence is measured after a 2–3 h incubation period using a microplate reader with the excitation/emission wavelength at (580/610 nm). The relative cell viability percentage was calculated using Eq. 3.

$$Relative\ Cell\ Viability\% = \frac{A\ test}{A\ control} \times 100 \quad (3)$$

Statistical analysis by Students Unpaired t test was carried out using GraphPad prism software for the cell viability experiments. The data was considered significant when $P < 0.05$.

2.12.   Immunofluorescence analysis

The downregulation of P-gp expression by CS-PEG-Bio-PLA NPs in the MDA-MB 453 breast cancer cells was studied using immunofluorescence staining method. MDA-MB 453 cells were sub-cultured and grown in glass-bottom dishes at a concentration of 5000–10 000 cells till confluent monolayer is achieved. The cells were then treated with a pre-determined concentration of Ver and CS-PEG-Bio-PLA NPs for 48 h. The treated cells were then washed thrice with $1 \times PBS$ buffer followed by their fixation with 4% paraformaldehyde for 20 min. The fixed cells were then permeabilized with cooled
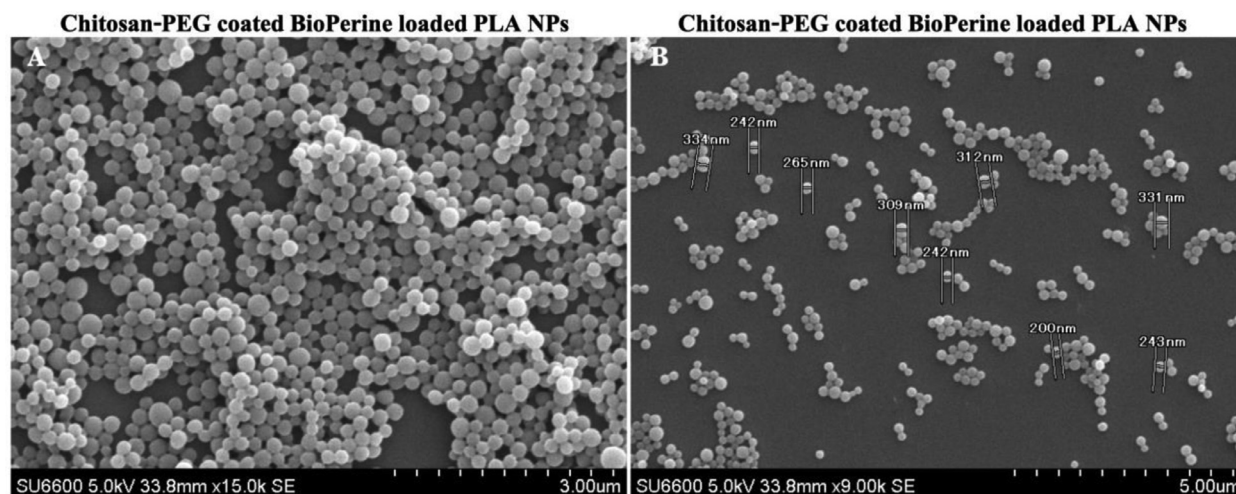
Figure 1 – SEM images of CS-PEG-Bio-PLA NPs at scale 3 μm and 5 μm.

methanol at -20 °C, followed by primary anti-P-gp antibody overnight incubation at 4 °C. In the next day, the cells were washed with $1 \times$ PBS buffer and then incubated with Alexa-594 secondary antibody for 45 min and then stained with NucBlue Live Ready Probes nuclear stain for 30 min. The cells are then imaged under the confocal microscope with the filter set appropriate for DAPI (Ex/Em: 425 nm/475 nm) and Cytidine 5 or Texas Red (Ex/Em: 570 nm/620 nm) laser channel.

2.13. Intracellular ROS activity by confocal microscopy

The intracellular reactive oxygen species was monitored using DCFDA/H2DCFDA assay kit which uses the cell-permeant 2',7'–dichlorofluorescein diacetate (DCFDA), a fluorogenic dye that measures hydroxyl, peroxyl and another ROS activity within the cell. For the assay, MDA-MB 453 cells were seeded in glass-bottom confocal dishes at a concentration of 5000–10,000 cells and grown till confluent. The cells were then treated with CS-PEG-Bio-PLA NPs alone and CS-PEG-Bio-PLA NPs plus Dox combination therapy at a pre-determined concentration for 24 h. Following the treatment, the cells were washed with $1 \times$ assay buffer and then incubated with 20-25 μM DCFDA dye for 30 min at 37 °C. The cells were washed with assay buffer and then imaged using a confocal microscope with the filter set appropriate for FITC laser channel (Ex/Em: 485 nm/535 nm).

3. Results and Discussion

3.1. Synthesis and characterization of CS-PEG-Bio-PLA NPs

CS-PEG-Bio-PLA NPs were observed to have smooth and spherical morphology similar to most polymeric NPs. The NPs as shown in Fig. 1A–1B recorded by SEM were in the range of 200-340 nm having an average size of 318.33 nm. The morphology of the NPs was also confirmed by TEM analysis (Fig. 2) illustrating a spherical shape with smooth surface.
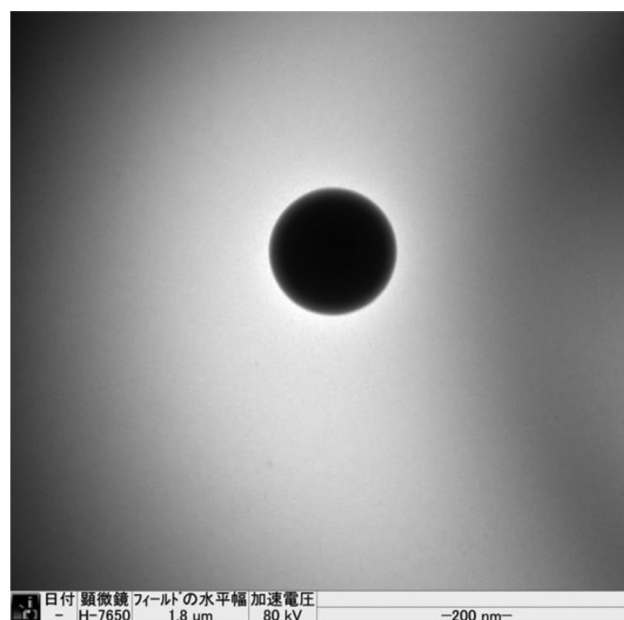

Figure 2 – TEM image of CS-PEG-Bio-PLA NPs at scale 200 nm.

From our size distribution analysis, we found out that the NPs ranged from 140–460 nm with a Z-average size of 316 nm as shown in Fig. 3 thus concurring with our SEM and TEM data. The zeta potential of the NPs was recorded to be +22.2 mV which could be due to the successful coating of both chitosan and PEG on the NPs leading to the increase in its zeta potential values. The encapsulation efficiency of BioPerine inside the CS-PEG-Bio-PLA NPs was found to be 98.42%.

The surface chemistry of CS-PEG-Bio-PLA NPs studied using XPS revealed the carbon (C) 1s and oxygen (O) 1s peak at 287 eV and 533 eV, respectively, thus confirming the presence of carbon and oxygen elements in the PLA polymer, PEG, BioPerine and chitosan which is also present
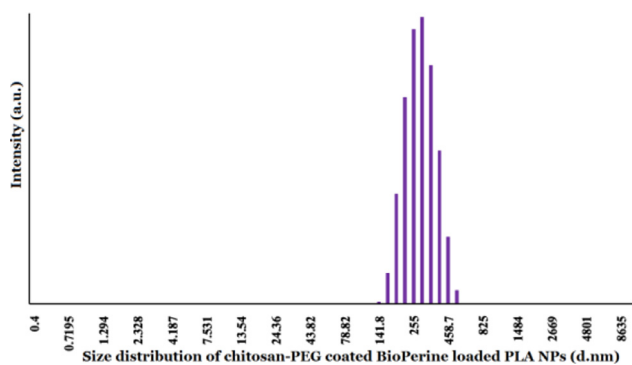
Figure 3 – Size distribution of CS-PEG-Bio-PLA NPs by DLS measurements.
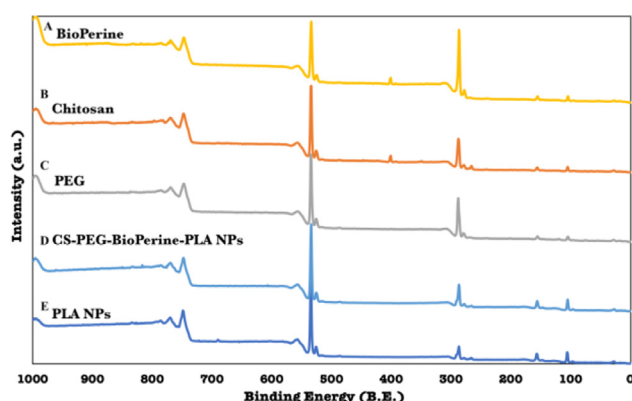

Figure 4 – XPS analysis of PLA NPs, Chitosan, PEG, BioPerine and CS-PEG-Bio-PLA NPs.

in these compounds as shown in the XPS spectra in Fig. 4.

We also carried out FTIR analysis to study the presence of functional groups and chemical interaction among the different components in the CS-PEG-Bio-PLA NPs as shown in Fig. 5. FTIR measurements of native chitosan as shown in Fig. 5A revealed characteristic band at 3346 cm^{-1} attributed to –NH$_2$ and –OH groups stretching vibration which is also mentioned in a previous study by Jain et al [36]. The spectra of void PLA NPs revealed characteristic peaks at 1747 cm^{-1} and 1080-1090 cm^{-1} due to C=O stretching and C–O–C stretching respectively as shown in Fig. 5B [37]. FTIR analysis of pure PEG was observed to have a –CH stretching vibration at 2879 cm^{-1} along with the distinct absorbance peaks at 1280 cm^{-1}, 955 cm^{-1} and 843 cm^{-1} as shown in Fig. 5C [38,39]. Native BioPerine spectra revealed the distinct peaks at 1635 cm^{-1} owing to –CO–N stretching and C=C (diene) symmetric and asymmetric stretching, 1580 cm^{-1} due to aromatic stretching of benzene ring, and 2939 cm^{-1} corresponds to C–H stretching vibrations as shown in Fig. 5D [40,41]. The confirmation of the successful encapsulation of BioPerine, surface coating of chitosan and PEG in the PLA NPs was revealed by the

characteristic peaks at 1635 cm^{-1} from BioPerine, 2993 cm^{-1} due to the amino groups from chitosan [31], and 955 cm^{-1} from PEG as shown in Fig. 5E. FTIR spectra of CS-PEG-Bio-PLA NPs revealed no appearance, no loss or shift in the major functional groups suggesting no strong chemical interactions among the drug and the polymers which could alter the functional and chemical characteristics of the components after nanoformulation. Individual spectrum of each sample as shown in Fig. S1. We also checked the possible interactions between BioPerine with PLA and BioPerine with chitosan by FTIR analysis. The spectra displayed there was no such interactions between them as shown in Fig. S2.

The nature of drug could be studied by XRD analysis that demonstrates the transition of its crystalline nature into its amorphous state after the nanoencapsulation process. The XRD patterns of pure PEG ($2\theta = 19.25°$, $23.5°$) [42] and pure chitosan ($2\theta = 20°$) [43] as shown in Fig. 6A and 6C revealed their major identification peaks depicting its crystalline nature which later changed into amorphous nature in CS-PEG-Bio-PLA NPs. From the XRD patterns of pure BioPerine as shown in Fig. 6B reveals strong reflection at $2\theta = 14.6°$, $22.5°$, $25.80°$ depicting the high crystalline nature of the drug. Conversely, the crystalline peaks of BioPerine disappeared in the CS-PEG-Bio-PLA NPs resembling the amorphous nature of the void PLA NPs as shown in Fig. 6D and 6E. The amorphization of crystalline drug inside the nanostructured system occurs probably due to the relatively higher solid-state drug-polymer solubility. This property influences the polymeric matrix to successfully entrap the drug molecular dispersion in the amorphous state which is evident from the broad bands of CS-PEG-BioPerine-PLA NPs compared to the diffraction peaks of free BioPerine [44]. Earlier studies also have reported such results where a purely crystalline drug changes into amorphous state in a nanostructured system [45].

3.2. In vitro BioPerine release

Polymeric drug delivery systems are known for their versatility in achieving controlled release profiles of any API encapsulated inside the core. For this study, we performed the *in vitro* drug release of BioPerine from NPs in a physiological pH 7.4 condition and also acidic condition pH 6.5 that mimics the tumor microenvironment with PBS buffer supplemented with FBS. We observed that BioPerine release from the CS-PEG-Bio-PLA NPs demonstrated a slow sustained release profile in pH 7.4 and increased BioPerine release in pH 6.5 over the 4 d study period. Within 24 h we observed 22.46% BioPerine release which increased to a maximum of only 25.58% on Day 4 as shown in the Fig. 7A in the physiological pH 7.4. While in acidic pH 6.5 we observed 27.06% to 36.35% release of BioPerine indicating a pH dependent release profile of the drug as shown in Fig. 7B that could be beneficial for the specific release in the tumor microenvironment to carry out its assigned activity and reduce cytotoxic effects in the normal tissues. This difference in rate of BioPerine release from the NPs core might be due to drug solubility, desorption of surface-bound drug, diffusion out of the NPs matrix into
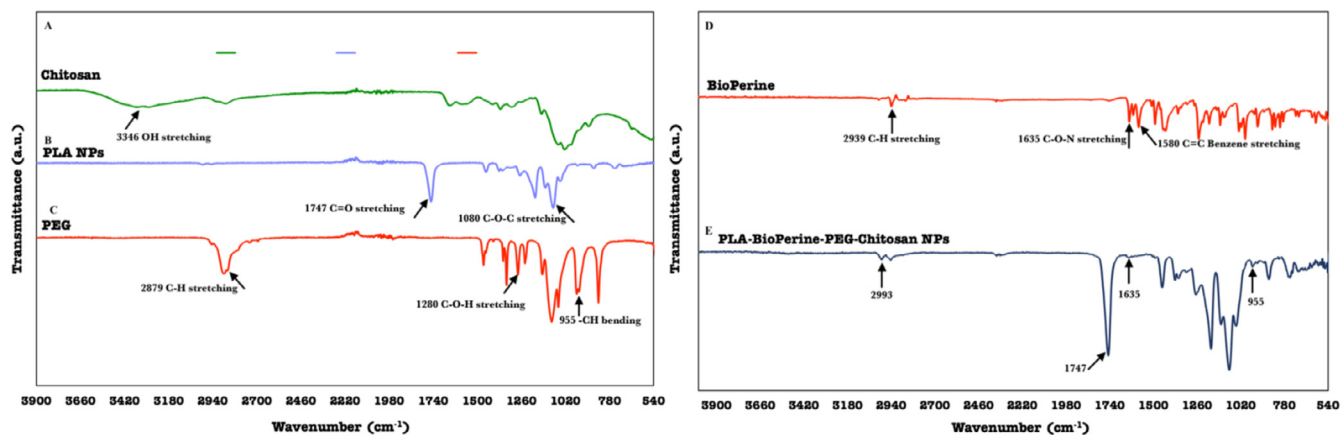
Figure 5 – ATR-FTIR analysis of Chitosan, PLA NPs, PEG, BioPerine and CS-PEG-Bio-PLA NPs in the range of 4000 to 400 cm^{-1}. (Individual spectrum provided in Fig. S1)
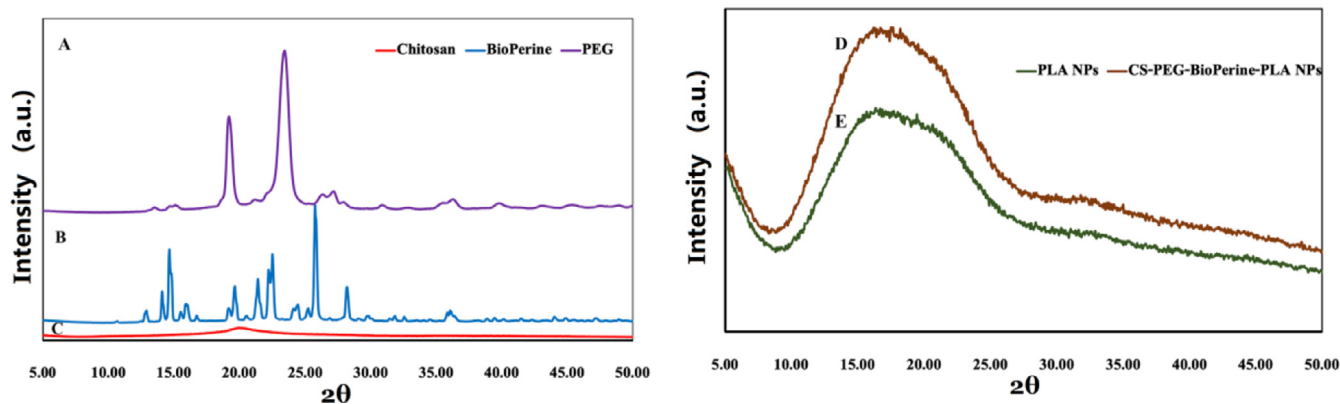

Figure 6 – Powder X-ray Diffraction patterns of (A) PEG, (B) BioPerine, (C) Chitosan, (D) CS-PEG-Bio-PLA NPs and (E) PLA NPs.
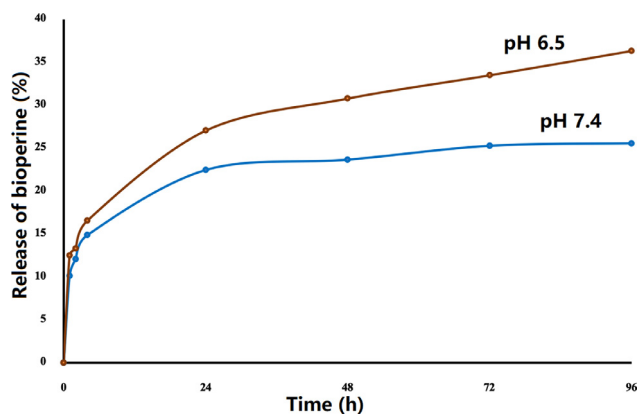

Figure 7 – *In vitro* BioPerine release from CS-PEG-Bio-PLA NPs in pH 7.4 (A) and pH 6.5 (B) PBS/FBS buffer studied over 4 d at 37 °C.

the body, NPs matrix erosion/degradation or a combination of both. We believe that the sustained release of BioPerine could be advantageous to achieve the longer circulation of the drug at a relatively low and safer concentration.

3.3. Intracellular uptake of CS-PEG-Coumarin 6-PLA NPs

The investigation on the intracellular uptake of NPs by the MDA-MB 453 cells was helmed by the synthesis of fluorescent dye coumarin 6-loaded CS-PEG-PLA NPs to trace the NPs fate in cells and tissues [46] by confocal microscopy. The nucleus was stained using a NucBlue probe (blue) and to mark the cellular membrane (actin filaments) phalloidin conjugate (red) dye was used. Upon incubating the MDA-MB 453 cells with the NPs for 4 h and 12 h we could observe a time-dependent uptake of the NPs as shown in the Fig. 7. After 4 h of incubation, we could observe the NPs attached to the cellular membrane, which could be due to the positive-negative interactions of the positively charged surface of NPs and the negative charged cellular membrane as shown in the Fig. 8A–8E. Hence, we decided to extend the incubation time to 12 h of the NPs. Due to extended incubation time of the NPs, we observed facilitated uptake as shown in Fig. 8F–8J thus confirming that MDA-MB 453 cells internalize NPs in a time-dependent manner and maximum influx of NPs could be speculated with a longer incubation period. Here we would like to point out that MDA-MB 231, which is another triple-negative breast cancer cell line was also shown to have maximum uptake of silibinin-loaded lipid
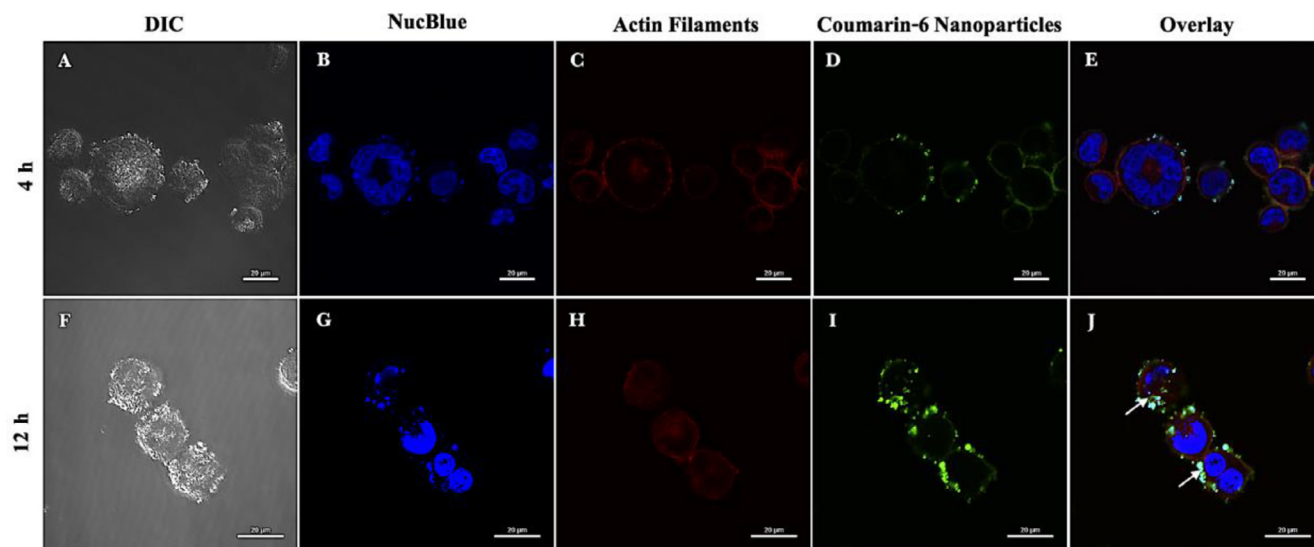
Figure 8 – Cellular uptake of Chitosan-PEG-Coumarin 6-PLA NPs in MDA-MB 453 triple-negative breast cancer cells for 4 h (A-E) and 12 h (F-J) (At scale 20 µm). Nuclei and actin filaments were stained using NucBlue Live Ready Probes and Phalloidin iFluor-647 dyes respectively to study NP co-localization.

NPs at 24 h compared to free silibinin which was around 6 h [47].

3.4.   *Relative cell viability by presto blue assay*

Inhibitory effects of CS-PEG-Bio-PLA NPs on MDA-MB 453 cells were examined by a dose and time-dependent study using the resazurin PrestoBlue assay. MDA-MB 453 cells were treated with 6 different concentrations of CS-PEG-Bio-PLA NPs for a period of 24–48 h. In comparison to the untreated cells (considered as 100% viable), we observed that the concentration ranging from (25, 50, 100 and 200 µg/ml) did not induce major inhibitory effects on the viability of the MDA-MB 453 cells at 24-h as shown in the Fig. 9. The cell viability at these concentrations were 83.56%, 80.82%, 67.12% and 67.12%, respectively. However, within 48 h we observed that the cell viability decreased in the above-mentioned concentrations from 55.55% to 54.16% as shown in the Fig. 10. MDA-MB 453 cells reacted better to the 500–1000 µg/ml concentration of CS-PEG-Bio-PLA NPs at both the periods, probably due to the therapeutic concentration of BioPerine encapsulated inside the NPs. The cell viability at these concentrations almost reduced to around 40% within 24–48 h as shown in the Fig. 9–10. We also observed that both 500 and 1000 µg/ml of CS-PEG-Bio-PLA NPs exerted inhibitory effects in the same range at both periods indicating that either of these two concentrations could potentially be used to induce P-gp inhibition in drug-resistant breast cancer. We further tested the cell viability of free BioPerine (5, 10, 25, 50, 100 and 150 µM) in the MDA-MB breast cancer cell line. From the cell viability studies of free BioPerine (Fig. S3) it was observed that the free BioPerine at a high concentration of 150 µM reduced the cell viability of the MDA-MB 453 breast cancer cells to a minimum of 25.48% at 48 h. The other concentrations of free BioPerine did not significantly reduce the cell viability of the breast cancer cells at all time points. The equivalent
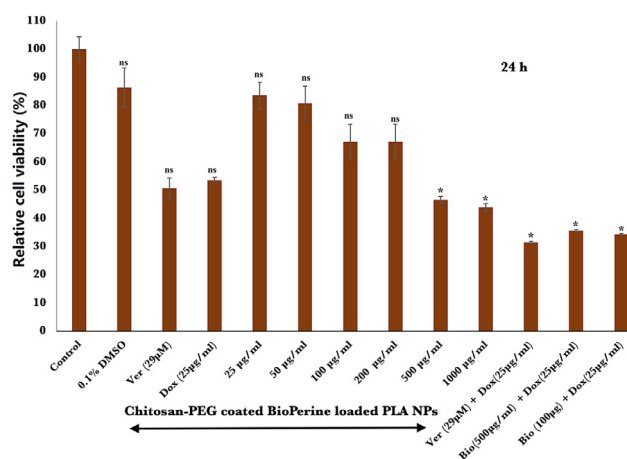

Figure 9 – Relative Cell viability of CS-PEG-Bio-PLA NPs, verapamil hydrochloride (Ver), doxorubicin (Dox), combination therapy of (Ver plus Dox and CS-PEG-Bio-PLA NPs plus Dox) in MDA-MB 453 triple-negative breast cancer cells at 24-h. Students Unpaired *t test* was carried out to check the statistical significance of the experiment (ns: not significant; *P < 0.05).

quantity of BioPerine encapsulated inside the CS-PEG-Bio-PLA NPs at the concentrations 500-1000 µg/ml was 23.49 µM and 50 µM, respectively which was sufficient enough to impart prolonged cytotoxicity to the cancer cells at such a mid-minimal concentration clearly indicating that delivery of BioPerine via the PLA-CS-PEG NPs is a better therapeutic strategy to target the drug-resistant breast cancer cells.

CS-PEG-Bio-PLA NPs were also compared with the commercial P-gp inhibitor Ver whose concentration was fixed at 29 µM from an earlier study conducted on breast cancer [48]. Ver at both periods (24–48 h) exerted inhibitory
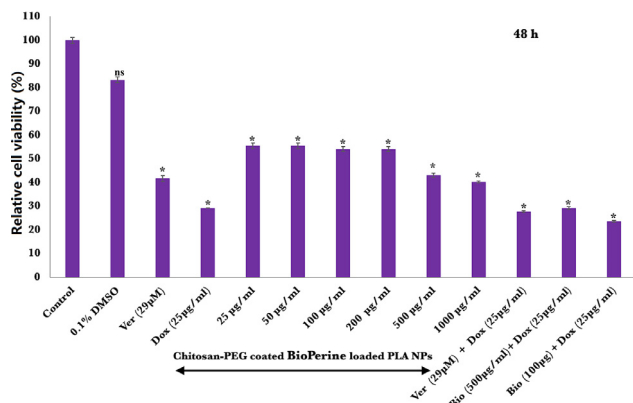
Figure 10 – Relative Cell viability of CS-PEG-Bio-PLA NPs, Ver, Dox, combination therapy of (Ver plus Dox and CS-PEG-Bio-PLA NPs plus Dox) in MDA-MB 453 triple-negative breast cancer cells at 48-h. Students Unpaired *t test* was carried out to check the statistical significance of the experiment (*ns*: not significant; *P < 0.05).

activity ranging from 50.68% to 41.66% as shown in the Fig. 9 and 10.

We also performed a combination strategy to check the enhanced killing of the MDA-MB 453 cells when pre-treated with CS-PEG-Bio-PLA NPs and Ver for 24 h followed by Dox administration for 24–48 h. Dox when administered as monotherapy to MDA-MB 453 cells, the cell viability reduced 53.42%-29.16% only within 24–48 h. When pre-treating the cells with the CS-PEG-Bio-PLA NPs and Ver, we observed that the cells when treated with 1000 μg/ml of CS-PEG-Bio-PLA NPs plus Dox exhibited better therapeutic efficacy than Ver plus Dox treatment within 48 h as shown in the Fig. 10. This establishes the fact that our CS-PEG-Bio-PLA NPs imparts improved cytotoxic activity towards the MDA-MB 453 cells not only as a monotherapy but also when combined with other conventional chemotherapy drugs.

3.5. P-gp expression by immunofluorescence analysis

Overexpression of ABC family of drug efflux transporters in multi-drug resistant cancers prevents the intracellular drug accumulation to therapeutic levels to perform anti-
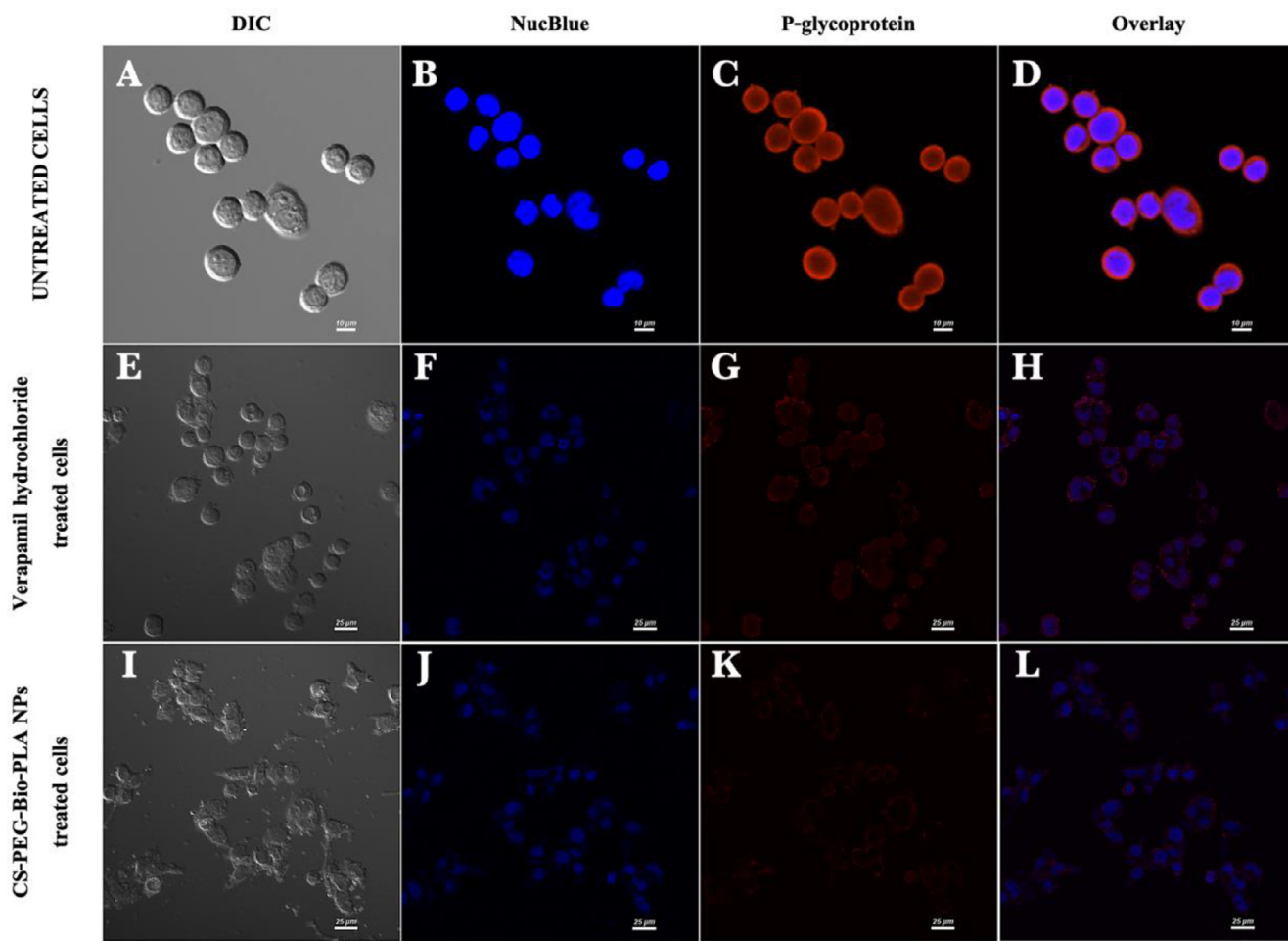

Figure 11 – Immunofluorescence analysis showing the expression of P-gp in untreated cells (A-D) and inhibition of P-gp expression in MDA-MB 453 cells upon treatment with verapamil hydrochloride (E-H) and CS-PEG-Bio-PLA NPs (I-L) for 48 h (At scale 10 μm and 25 μm).
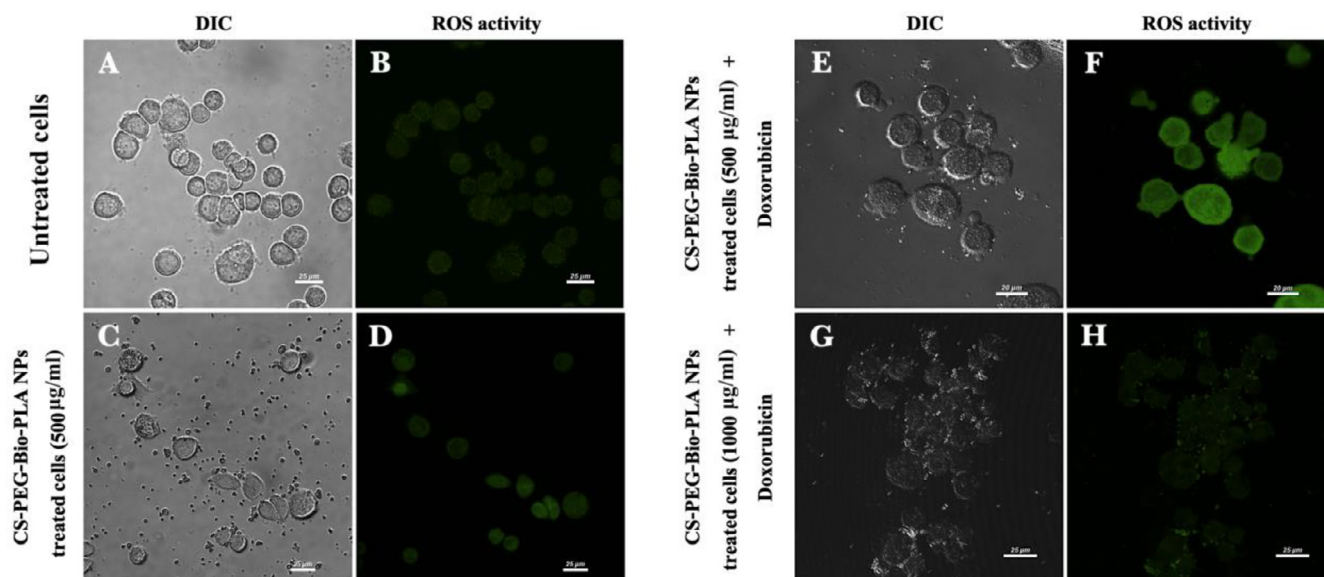
Figure 12 – Cellular ROS levels in MDA-MB 453 cells evaluated using DCFDA/H2DCFDA assay dye kit (2'7' dichlorofluorescein diacetate) by confocal microscopy. (A-B) Untreated cells, (C-D) MDA-MB 453 cells upon treatment with CS-PEG-Bio-PLA NPs, (E-F) MDA-MB 453 cells upon treatment with CS-PEG-Bio-PLA NPs (500 μg/ml) plus Dox (25 μg/ml), (G-H) MDA-MB 453 cells upon treatment with CS-PEG-Bio-PLA NPs (1000 μg/ml) plus Dox (25 μg/ml) (At scale 20 μm and 25 μm).

cancer activities. P-gp is one of the best-studied drug efflux pumps in this family of transporters that mediate the reduced accumulation of various chemotherapeutic drugs finally leading to resistance in breast [49] and ovarian cancers [50]. The inhibition of the P-gp expression in the MDA-MB 453 cells by the CS-PEG-Bio-PLA NPs was studied and compared with the commercial P-gp inhibitor Ver by immunofluorescence staining. The untreated cells displayed an overtly high expression of P-gp on the cellular membrane as shown in Fig. 11A–11D while the Ver treated cells displayed reduction in the P-gp expression within 48 h as shown in Fig. 11E–11H, respectively. CS-PEG-Bio-PLA NPs treated cells displayed further reduction in the P-gp expression in the MDA-MB 453 cells within 48 h as seen in Fig. 12I–12L thus corroborating the fact the downregulation of P-gp by BioPerine might lead to improved accumulation of Dox in the drug-resistant breast cancer cells mediating their increase killing efficacy. The delivery of BioPerine via the hybrid PLA NPs would lead to sustained downregulation of P-gp activity in multi-drug resistant cancers cells while elevating the intracellular levels of chemotherapeutics for enhanced therapeutic efficacy.

3.6.   Intracellular ROS activity

Increased ROS levels impart redox imbalance in cancer cells due to high metabolic rate and mitochondrial dysfunction in comparison to normal cells which surges cancer cells towards increased oxidative stress. An induction to additional oxidative stress in cancer cells might lead to oxidative stress-induced cell death [51]. Several dietary compounds such as polyphenols [52] and flavonoids are shown to increase the ROS levels in cancer cells and mediates killing by inhibiting cell proliferation and inducing autophagy and apoptosis. We

intend to study the induction of ROS levels in the MDA-MB 453 cells by the CS-PEG-Bio-PLA NPs (500 μg/ml) when treated for 24 h. The untreated MDA-MB 453 cells did not produce a surge in ROS levels as shown in Fig. 12A–12B. The MDA-MB 453 cells upon incubation with CS-PEG-Bio-PLA NPs alone for 24 h revealed a slight increase in the ROS levels as shown in Fig. 12C–12D. However, we did observe an increased surge in ROS levels in the MDA-MB 453 cells when treated with the same concentration of CS-PEG-Bio-PLA NPs (500 μg/ml) plus Dox (25 μg/ml) as a combination therapy as shown in Fig. 12E–12F. We also observed that the cells when treated with combination therapy of CS-PEG-Bio-PLA NPs at 1000 μg/ml plus Dox (25 μg/ml) ROS levels dropped to a minimum level as shown in Fig. 12G–12H suggesting that ROS activity in cells is dose-dependent. We speculated that a concentration of 500 μg/ml CS-PEG-Bio-PLA NPs with a combination therapy of Dox would be appropriate to induce ROS levels in the MDA-MB 453 drug-resistant cancer cells and mediate its cellular death within 24 h which we noticed in the cell viability studies both monotherapy (CS-PEG-Bio-PLA NPs) and combination therapy (CS-PEG-Bio-PLA NPs plus Dox).

4.   Conclusion

This study concluded the successful fabrication of BioPerine-loaded PLA NPs surface coated with chitosan and PEG (CS-PEG-Bio-PLA NPs) that improved its aqueous solubility and imparted sustained BioPerine release. The positively charged CS-PEG-Bio-PLA NPs having a smooth spherical morphology were also successfully internalized by the MDA-MB 453 breast cancer cells within 12-h owing to the positive-negative interactions between the NPs and the cellular

membrane. CS-PEG-Bio-PLA NPs exhibited a pH-dependent release profile of BioPerine which will be beneficial for achieving controlled release at the acidic tumor tissues and spare the normal tissues having a neutral pH. This sustained release of BioPerine from the NPs will impart prolonged P-gp inhibition as evident from the immunofluorescence analysis and also enhanced cytotoxicity at 48 h in comparison to the commercial inhibitor verapamil hydrochloride. Notably, our findings also demonstrated the induction of reactive oxygen species levels in MDA-MB 453 cells when treated with the CS-PEG-Bio-PLA NPs alone and with Dox as a combination therapy suggesting dose-dependent ROS induction to mediate cell death. We anticipate that the CS-PEG-Bio-PLA NPs could also be harnessed to co-deliver anti-cancer compounds of interest for a more efficient anti-cancer therapy against a wide range of P-gp expressing drug-resistant cancers in future scenarios.

Conflicts of interest

The authors declare no conflict of interest.

Acknowledgements

Supplementary materials

Supplementary material associated with this article can be found, in the online version, at doi:10.1016/j.ajps.2020.04.001.

REFERENCES

[1] Musgrove EA, Sutherland RL. Biological determinants of endocrine resistance in breast cancer. Nat Rev Cancer 2009;9(9):631–43.

[2] Gonzalez-Angulo AM, Morales-Vasquez F, Hortobagyi GN. Overview of resistance to systemic therapy in patients with breast cancer. In: Yu D, Huang MC, editors. Breast cancer chemosensitivity. Advances in experimental medicine and biology, vol608. New York: Springer; 2007. p. 1–22.

[3] Guiu S, Michiels S, André F, Andre F, Cortes J, Denkert C, Di Leo A, et al. Molecular subclasses of breast cancer: how do we define them? The IMPAKT 2012 working group statement. Annals of oncology 2012;23(12):2997–3006.

[4] Lim E, Metzger-Filho O, Winer EP. The natural history of hormone receptor-positive breast cancer. Oncology 2012;26(8):688–94.

[5] Nahta R, O'Regan RM. Therapeutic implications of estrogen receptor signaling in HER2-positive breast cancers. Breast Cance Res Treat 2012;135(1):39–48.

[6] Vu T, Claret FX. Trastuzumab: updated mechanisms of action and resistance in breast cancer. Frontiers in oncology 2012;2:62.

[7] Hudis CA, Gianni L. Triple-negative breast cancer: an unmet medical need. Oncologist 2011;16(Suppl 1):1–11.

[8] Clarke R, Leonessa F, Trock B. Multidrug resistance/P-glycoprotein and breast cancer: review and meta-analysis. Semin Oncol 2005;32(Suppl 7):S9–15.

[9] Wind NS, Holen I. Multidrug resistance in breast cancer: from in vitro models to clinical studies. Int J Breast Cancer 2011;2011:967419.

[10] Nobili S, Landini I, Mazzei T, Mini E. Overcoming tumor multidrug resistance using drugs able to evade P-glycoprotein or to exploit its expression. Med Res Rev 2012;32(6):1220–62.

[11] Callaghan R, Luk F, Bebawy M. Inhibition of the multidrug resistance P-glycoprotein: time for a change of strategy? Drug Metab Dispos 2014;42(4):623–31.

[12] Nanayakkara AK, Follit CA, Chen G, Williams NS, Vogel PD, Wise JG. Targeted inhibitors of P-glycoprotein increase chemotherapeutic-induced mortality of multidrug resistant tumor cells. Sci Rep 2018;8(1):1–8.

[13] Khan M, Maryam A, Mehmood T, Zhang Y, Ma T. Enhancing activity of anticancer drugs in multidrug resistant tumors by modulating p-glycoprotein through dietary nutraceuticals. Asian Pacific J Cancer Prev 2015;16(16):6831–9.

[14] Han Y, Chin Tan TM, Lim LY. In vitro and in vivo evaluation of the effects of piperine on P-gp function and expression. Toxicol Appl Pharmacol 2008;230(3):283-9.

[15] Bezerra DP, De Castro FO, Alves APNN, Pessoa C, Moraes MO, Silveira ER, et al. In vitro and in vivo antitumor effect of 5-FU combined with piplartine and piperine. J Appl Toxicol 2008;28(2):156–63.

[16] Bang JS, Oh DH, Choi HM, Sur BJ, Lim SJ, Kim JY, et al. Anti-inflammatory and antiarthritic effects of piperine in human interleukin 1β-stimulate fibroblast-like synoviocytes and in rat arthritis models. Arthritis Res Ther 2009;11(2):R49.

[17] Bhutani MK, Bishnoi M, Kulkarni SK. Anti-depressant like effect of curcumin and its combination with piperine in unpredicable chronic stress-induced behavioral, biochemical and neurochemical changes. Pharmacol Biochem Behav 2009;92(1):39–43.

[18] Li CR, Wang ZJ, Wang Q, Ka Yan Ho RL, Huang Y, Chow MSS, et al. Enhanced anti-tumor efficacy and mechanisms associated with docetaxel-piperine combination- in vitro and in vivo investigation using a taxane-resistant prostate cancer model. Oncotarget 2018;9(3):3338–52.

[19] Baspinar Y, Üstündas M, Bayraktar O, Sezgin C. Curcumin and piperine loaded zein-chitosan nanoparticles: development and in vitro characterisation. Saudi Pharm J 2018 Mar 1;26(3):323–34.

[20] Katiyar SS, Muntimadugu E, Rafeeqi TA, Domb AJ, Khan W. Co-delivery of rapamycin- and piperine-loaded polymeric nanoparticles for breast cancer treatment. Drug Deliv 2016;23(7):2608–16.

[21] Gorgani L, Mohammadi M, Najafpour GD, Nikzad M. Piperine—the bioactive compound of black pepper: from isolation to medicinal formulations. Compr Rev Food Sci Food Saf 2017;16(1):124–40.

[22] Lee SH, Kim HY, Back SY, Han HK. Piperine-mediated drug interactions and formulation strategy for piperine: recent advancs and future perspectives. Expert Opin Drug Metab Toxicol 2018;14(1):43–57.

[23] Lassalle V, Ferreira ML. PLA nano- and microparticles for drug delivery: an overview of the methods of preparation. Macromol Biosci 2007;7(6):767–83.

[24] Madhavan Nampoothiri K, Nair NR, John RP. An overview of the recent developments in polylactide (PLA) research. Bioresour Technol 2010;101(22):8493–501.

[25] Lee BK, Yun Y, Park K. PLA micro- and nano-particles. Adv Drug Deliv Rev 2016;107:176–91.

[26] Mahapatro A, Singh DK. Biodegradable nanoparticles are excellent vehicle for site directed *in vivo* delivery of drugs and vaccines. J Nanobiotechnology 2011;9(1):55.

[27] Kamaly N, Xiao Z, Valencia PM, Radovic-Moreno AF, Farokhzad OC. Targeted polymeric therapeutic nanoparticles: design, development and clinical translation. Chem Soc Rev 2012;41(7):2971–3010.

[28] Hu FQ, Meng P, Dai YQ, Du YZ, You J, Wei XH, et al. PEGylated chitosan-based polymer micelle as an intracellular delivery carrier for anti-tumo targeting therapy. Eur J Pharm Biopharm 2008;70(3):749–57.

[29] Illum L. Chitosan and its use as a pharmaceutical excipient. Pharm Res 1998;15(9):1326–31.

[30] Otsuka H, Nagasaki Y, Kataoka K. PEGylated nanoparticles for biological and pharmaceutical applications. Adv Drug Deliv Rev 2003;55(3):403–19.

[31] Parveen S, Sahoo SK. Long circulating chitosan/PEG blended PLGA nanoparticle for tumor drug delivery. Eur J Pharmacol 2011 Nov 30;670(2-3):372–83.

[32] Ince P, Appleton DR, Finney KJ, Sunter JP, Watson AJ. Verapamil increases the sensitivity of primary human colorectal carinoma tissue to vincristine. Br J Cancer 1986;53(1):137.

[33] Merry S, Fetherston CA, Kaye SB, Freshney RI, Plumb JA. Resistance of human glioma to adriamycin *in vitro*: the role of membrane transport and its circumvention with verapamil. Br J Cancer 1986;53(1):129–35.

[34] Amini Y, Amel Jamehdar S, Sadri K, Zare S, Musavi D, Tafaghodi M. Different methods to determine the encapsulation efficincy of protein in PLGA nanoparticles. Biomed Mater Eng 2017;28(6):613–20.

[35] Kibria G, Hatakeyama H, Akiyama K, Hida K, Harashima H. Comparative study of the sensitivities of cancer cells to doxorubicin, and relationships between the effect of the drug-efflux pump P-gp. Biol Pharm Bull 2014;37(12):1926–35.

[36] Jain D, Banerjee R. Comparison of ciprofloxacin hydrochloride-loaded protein, lipid, and chitosan nanoparticles for drug delivery. J Biomed Mater Res-Part B Appl Biomater 2008;86(1):105–12.

[37] Yuniarto K, Purwanto YA, Purwanto S, Welt BA, Purwadaria HK, Sunarti TC. Infrared and Raman studies on polylactide acid and polyethylene glycol-400 blend. AIP Conference Proceedings 2016;1725(1) 020101).

[38] Kolhe P, Kannan RM. Improvement in ductility of chitosan through blending and copolymerization with PEG: FTIR investigation of molecular interactions. Biomacromolecules 2003;4(1):173–80.

[39] Venkatasubbu GD, Ramasamy S, Avadhani GS, Ramakrishnan V, Kumar J. Surface modification and paclitaxel drug delivery of folic acid modified polyethylene glycol functionalized hydroxyapatite nanoparticles. Powder Technol 2013 Feb 1;235:437–42.

[40] Gorgani L, Mohammadi M, Najafpour GD, Nikzad M. Sequential microwave-ultrasound-assisted extraction for isolation of piperine from black pepper (Piper nigrum L.). Food Bioprocess Technol 2017;10(12):2199–207.

[41] Pachauri M, Gupta ED, Ghosh PC. Piperine loaded PEG-PLGA nanoparticles: Preparation, characterization and targeted delivery for adjuvant breast cancer chemotherapy. J Drug Deliv Sci Technol 2015;29:269–82.

[42] Pramanik S, Ataollahi F, Pingguan-Murphy B, Oshkour AA, Osman NAA. *In vitro* study of surface modified poly(ethylene glycol)-impregnated sintered bovine bone scaffolds on human fibroblast cells. Sci Rep 2015;5:9806.

[43] Kumar S, Koh J. Physiochemical, optical and biological activity of chitosan-chromone derivative for biomedical applications. Int J Mol Sci 2012;13(5):6102–16.

[44] Panyam J, Williams D, Dash A, Leslie-Pelecky D, Labhasetwar V. Solid-state solubility influences encapsulation and release of hydrophobic drugs from PLGA/PLA nanoparticles. J Pharm Sci 2004;93(7):1804–14.

[45] Moraes Moreira Carraro TC, Altmeyer C, Maissar Khalil N, Mara Mainardes R. Assessment of *in vitro* antifungal efficacy and *in vivo* toxicity of Amphotericin B-loaded PLGA and PLGA-PEG blend nanoparticles. J Mycol Med 2017;27(4):519–29.

[46] Chung JW, Lee K, Neikirk C, Nelson CM, Priestley RD. Photoresponsive coumarin-stabilized polymeric nanoparticles as a detectable drug carrier. Small 2012;8(11):1693–700.

[47] Xu P, Yin Q, Shen J, Chen L, Yu H, Zhang Z, et al. Synergistic inhibition of breast cancer metastasis by silibinin-loaded lipid nanoparticles containing TPGS. Int J Pharm 2013;454(1):21–30.

[48] Correia A, Silva D, Correia A, Vilanova M, Gärtner F, Vale N. Study of new therapeutic strategies to combat breast cancer using drug combinations. Biomolecules 2018;8(4):175.

[49] Mechetner E, Kyshtoobayeva A, Zonis S, Kim H, Stroup R, Garcia R, et al. Levels of multidrug resistance (MDR1) P-glycoprotein expression by human breast cancer correlate with *in vitro* resistance to taxol and doxorubicin. Clin Cancer Res 1998;4(2):389–98.

[50] Penson RT, Oliva E, Skates SJ, Glyptis T, Fuller AF Jr, Goodman A, et al. Expression of multidrug resistance-1 protein inversely correlates with paclitaxel response and survival in ovarian cancer patients: A study in serial samples. Gynecol oncol 2004;93(1):98–106.

[51] Trachootham D, Alexandre J, Huang P. Targeting cancer cells by ROS-mediated mechanisms: a radical therapeutic approach? Nat Rev Drug Discov 2009;8(7):579–91.

[52] Mileo AM, Miccadei S. Polyphenols as modulator of oxidative stress in cancer disease: new therapeutic strategies. Oxid Med Cell Longev 2016;2016:6475624.